Journal of Sound and Vibration (1999) **220**(4), 625–640
Article No. jsvi.1998.1932, available online at http://www.idealibrary.com on IDEAL

DEVELOPMENT OF AN AUTOMOTIVE JOINT MODEL USING AN ANALYTICALLY BASED FORMULATION

Y.-M. MOON

University of Michigan, Ann Arbor, 48109, *MI, U.S.A.*

T.-H. JEE

Functional Test Team 2, *Passenger Car R&D Center* 2, *Hyundai Motor Company, Korea*

AND

Y.-P. PARK

Mechanical Engineering Faculty, Yonsei University, Seoul, Korea

(*Received* 16 *June* 1997, *and in final form* 6 *August* 1998)

A FE model of an automotive structure consists of beam and shell elements. Generally, the pillars and rockers are modelled as beam elements and other parts as shell elements. Beam elements are used since they are more efficient than shell elements. A joint is defined as an intersection region of beam elements, and is generally modelled as coupled rotational springs. In this study, a joint modelling methodology is presented. First, the definition and assumptions of the joint are discussed. Second, the joint stiffness analytical model is proposed using static load test results. The proposed method is more efficient and accurate than existing evaluation methods. Third, the sensitivity analysis method (Nelson's method) and a joint stiffness updating algorithm are presented. To verify these methods, the FE analysis results of a half size structural model of an automobile with rigid joints and rotational spring joints are compared with experimental modal analysis results.

© 1999 Academic Press

1. INTRODUCTION

In order to predict static and dynamic responses of automotive structures, a FE (Finite Element) method is often used. A FE representation of the automotive structure should be modelled by shell elements since most passenger cars are composed of steel plates. The shell element model, however, requires more memory and computer time than that of beam elements. Therefore, the shell element model is not efficient for conceptual design of an automotive structure in which frequent model changes are required. Thus, beam-shaped parts such as rockers, pillars, etc., are modelled using beam elements to improve computational

0022–460X/99/090625 + 16 $30.00/0 © 1999 Academic Press

efficiency. Since these beam-shaped parts carry major portions of the automotive structural loads, it is important to analyze joints at the intersections of beam to beam or beam to plate. Special considerations are needed in joint modelling, because it can deform locally. Previous automotive structural analyses considered joints as rigid connections. However, those models inaccurately described static and dynamic automotive structure behavior.

In the early 70's, using a 2-D structural model with rotational spring joint, Chang [1] showed that joint flexibility could not be neglected. After this study, a rotational spring model of a joint was generally accepted. Chon [2] verified the joint spring sensitivity with respect to the whole strain energy of the automotive structure. If a joint stiffness exceeds the threshold value, then the total strain energy of the structure becomes insensitive to the particular joint. Chon demonstrated the above phenomena theoretically by showing that the derivative of the total strain energy with respect to a particular joint stiffness decreases and becomes zero as the joint stiffness approaches infinity. Sakurai and Kamada [3] studied T-shaped joints consisting of box beams. Shimomaki *et al*. [4] presented a joint stiffness matrix using a 3-D FE model which has rigid beam and 3-DOF (degrees of freedom) rotational spring elements. The authors showed that the characteristics of the joint stiffness can be evaluated by eigenvalues and eigenvectors of a sub-matrix and also used joint stiffness ellipsoids. Lee [5] presented a general joint modelling methodology and introduced the basic assumptions that the behavior of a joint is linear elastic and the joint branches are rigidly connected in translation.

The sensitivity analysis method has been studied as a method for estimating the importance of design variables and updating analytic models. Fox and Kapoor [6] presented a sensitivity analysis method in which eigenvector derivatives are expanded in terms of the modal coordinates. Sohn [7] proposed a modified method that is based upon sensitivity analysis of natural frequencies and natural modes. Sohn used the sensitivity analysis method to estimate structural variables such as Young's modulus and material density. Nelson [8] presented a simple and fast method to calculate an eigenvector derivative. Lim [9] compared Fox's and Nelson's methods.

In this study, an automotive structure joint is defined and a general 3-branched joint is considered. The new joint stiffness evaluation method uses static load test data, which until now has not been analytically possible due to the coupling effect. Joint stiffness values obtained from this method are compared with stiffness values obtained from sensitivity analysis using Nelson's [8] eigenvector derivative. Dynamic characteristics of joint models using each stiffness value are compared with that of a rigid joint. To verify this methodology, a half size automotive structural model was fabricated and analyzed.

2. ANALYTICAL SOLUTION OF THE JOINT STIFFNESS

2.1. JOINT MODELLING

An automotive structure joint is defined as a region in which there is an abrupt change in geometric continuity. In an automotive structure (passenger cars), the

joints represent the intersection regions of rocker and center pillar, roof rail and center pillar, roof rail and windshield pillar, and so on. Shimomaki *et al*. [4] show that the off-diagonal terms of the joint stiffness matrix are only 0·1% the magnitude of the diagonal terms. The off-diagonal terms are therefore deemed negligible. Total joint mass is less than 5% of roof rail mass or center pillar mass in a real automotive structure, and 2% of that in the model car. Thus its effect is also negligible. Based on this discussion, the following assumptions are used in joint modelling.

1. The joint branches are rigidly connected with respect to translational motion, and their displacements are only due to rotational spring stiffness.
2. In the stiffness matrix, there is no coupling between co-ordinates.
3. The joints are weightless.

The typical 3-branched joint is generally a Y-type joint. The branches are modelled as rigid beams, and the joints are modelled as sets of rotational springs. Figure 1 shows the Y-type joint shape, where the springs have 3 rotational-DOF with stiffness about X-, Y- and Z-axes. Equation (1) describes the matrix form of joint stiffness

$$\begin{bmatrix} [\mathbf{K}_b]+[\mathbf{K}_c] & -[\mathbf{K}_c] & -[\mathbf{K}_b] \\ -[\mathbf{K}_c] & [\mathbf{K}_c]+[\mathbf{K}_a] & -[\mathbf{K}_a] \\ -[\mathbf{K}_b] & -[\mathbf{K}_a] & [\mathbf{K}_a]+[\mathbf{K}_b] \end{bmatrix} \begin{Bmatrix} \{\mathbf{\Theta}_1\} \\ \{\mathbf{\Theta}_2\} \\ \{\mathbf{\Theta}_3\} \end{Bmatrix} = \begin{Bmatrix} \{\mathbf{M}_1\} \\ \{\mathbf{M}_2\} \\ \{\mathbf{M}_3\} \end{Bmatrix}, \tag{1}$$

where, $[\mathbf{K}_i]$ is joint stiffness matrix, $\{\mathbf{\Theta}_i\}$ is displacement vector, $\{\mathbf{M}_i\}$ is moment vector as below.

$$[\mathbf{K}_i] = \begin{bmatrix} K_{ix} & 0 & 0 \\ 0 & K_{iy} & 0 \\ 0 & 0 & K_{iz} \end{bmatrix}, \quad i = a, b, c, \qquad \{\mathbf{\Theta}_i\} = \begin{Bmatrix} \mathbf{\Theta}_{ix} \\ \mathbf{\Theta}_{iy} \\ \mathbf{\Theta}_{iz} \end{Bmatrix},$$

$$\{\mathbf{M}_i\} = \begin{Bmatrix} \mathbf{M}_{ix} \\ \mathbf{M}_{iy} \\ \mathbf{M}_{iz} \end{Bmatrix}, \quad i = 1, 2, 3.$$

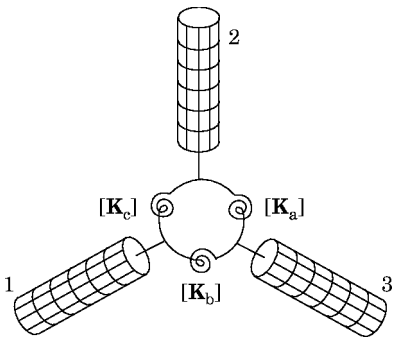

Figure 1. Rotational spring joint model of Y-type joint.

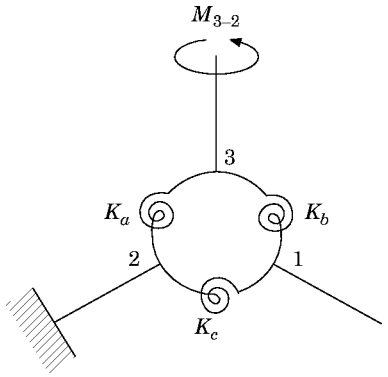

Figure 2. Rotational spring joint model with applied static moment.

2.2. ANALYTICAL SOLUTION

In equation (1), it is impossible to calculate the stiffness value by using measured moments and rotational displacements. Therefore, in this study, a method for calculating stiffness matrix coefficients from experimental data (namely static load test data) is proposed. To simplify the 3-D plane joint model shown in Figure 1, it is assumed that a 3-DOF rotational spring is regarded as a 1-DOF spring. Each branch is a rigid beam that cannot deflect or twist and the rotational displacement only occurs at the joint spring by the applied moment. To solve this simplified 1-D plane model, consider boundary condition where branch 2 is fixed and branch 3 is subjected to an applied moment as shown in Figure 2. In Figure 2, the displacement and moment are $\mathbf{\Theta}_{3-2}$ and M_{3-2}, respectively. The model in Figure 2 can also be represented as the equivalent translational spring model of Figure 3 and first part of equation (2). Therefore, the stiffness value of the model shown in Figure 3 is the first part of equation (2), where subscript $3-2$ means that branch 2 is fixed and branch 3 is subjected to an applied moment. Next, change the boundary and load conditions, to complete the remaining parts of equation (2).

$$(K_a + K_b K_c/(K_b + K_c))\mathbf{\Theta}_{3-2} = M_{3-2}, \qquad (K_b + K_c K_a/(K_c + K_a))\mathbf{\Theta}_{1-3} = M_{1-3},$$

$$(K_c + K_a K_b/(K_a + K_b))\mathbf{\Theta}_{2-1} = M_{2-1}. \tag{2}$$

To solve these simultaneous equations, three variables are defined

$$\alpha \equiv M_{3-2}/\mathbf{\Theta}_{3-2}, \qquad \beta \equiv M_{1-3}/\mathbf{\Theta}_{1-3}, \qquad \gamma \equiv M_{2-1}/\mathbf{\Theta}_{2-1}. \tag{3}$$

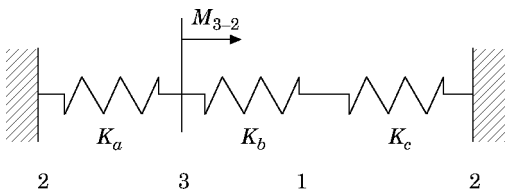

Figure 3. Equivalent translational spring model.

Substituting equation (3) into equation (2) gives

$$(K_a + K_b K_c/(K_b + K_c)) = \alpha, \qquad (K_b + K_c K_a/(K_c + K_a)) = \beta,$$
$$(K_c + K_a K_b/(K_a + K_b)) = \gamma. \tag{4}$$

Rewriting equation (4)

$$K_a K_b + K_b K_c + K_c K_a = (K_b + K_c)\alpha,$$
$$K_a K_b + K_b K_c + K_c K_a = (K_c + K_a)\beta, \qquad K_a K_b + K_b K_c + K_c K_a = (K_a + K_b)\gamma, \tag{5}$$

Solving equation (5), one has the analytical stiffness values

$$K_c = [(-\alpha\beta + \beta\gamma + \gamma\alpha)/(\alpha\beta - \beta\gamma + \gamma\alpha)]K_a = n_1 K_a,$$
$$K_b = [(\alpha\beta + \beta\gamma - \gamma\alpha)/(\alpha\beta - \beta\gamma + \gamma\alpha)]K_a = n_2 K_a, \tag{6, 7}$$
$$K_a = (n_1 + n_2)\alpha/(n_1 n_2 + n_2 + n_1) = (1 + n_1)\beta/(n_1 n_2 + n_2 + n_1),$$
$$= (1 + n_2)\gamma/(n_1 n_2 + n_2 + n_1). \tag{8}$$

It is possible to calculate the stiffness values of another plane of Figure 1 in the same manner. After obtaining moment and rotational displacement by the static load test, stiffness values of each joint are acquired by substituting equations (6)–(8).

2.3. SENSITIVITY ANALYSIS—EIGENVALUE DERIVATIVE

The equation of motion for an n-DOF system without damping is

$$[\mathbf{M}]\{\ddot{\mathbf{x}}\} + [\mathbf{K}]\{\mathbf{x}\} = \{\mathbf{F}\}, \tag{9}$$

where $[\mathbf{M}]$ and $[\mathbf{K}]$ are $n \times n$ mass and stiffness matrices, $\{\mathbf{x}\}$ and $\{\mathbf{F}\}$ are n-dimensional displacement and applied force vectors respectively. The eigenvalue problem of equation (9) is

$$([\mathbf{K}] - \lambda_r[\mathbf{M}])\{\boldsymbol{\phi}\}_r = \{\mathbf{0}\}, \tag{10}$$

where λ_r is the rth eigenvalue and $\{\boldsymbol{\phi}\}_r$ is the rth eigenvector. Taking the partial derivative of equation (10) with respect to structural variable P_i $(i = 1, \ldots, N)$ gives

$$\left(\frac{\partial[\mathbf{K}]}{\partial P_i} - \lambda_r \frac{\partial[\mathbf{M}]}{\partial P_i}\right)\{\boldsymbol{\phi}\}_r - \frac{\partial \lambda_r}{\partial P_i}[\mathbf{M}]\{\boldsymbol{\phi}\}_r + ([\mathbf{K}] - \lambda_r[\mathbf{M}])\frac{\partial\{\boldsymbol{\phi}\}_r}{\partial P_i} = \{\mathbf{0}\}. \tag{11}$$

Premultiplying of equation (11) by $\{\boldsymbol{\phi}\}_r^{\mathrm{T}}$ gives

$$\{\boldsymbol{\phi}\}_r^{\mathrm{T}}\left(\frac{\partial[\mathbf{K}]}{\partial P_i} - \lambda_r \frac{\partial[\mathbf{M}]}{\partial P_i}\right)\{\boldsymbol{\phi}\}_r - \frac{\partial \lambda_r}{\partial P_i}\{\boldsymbol{\phi}\}_r^{\mathrm{T}}[\mathbf{M}]\{\boldsymbol{\phi}\}_r$$
$$+ \{\boldsymbol{\phi}\}_r^{\mathrm{T}}([\mathbf{K}] - \lambda_r[\mathbf{M}])\frac{\partial\{\boldsymbol{\phi}\}_r}{\partial P_i} = \{\mathbf{0}\}. \tag{12}$$

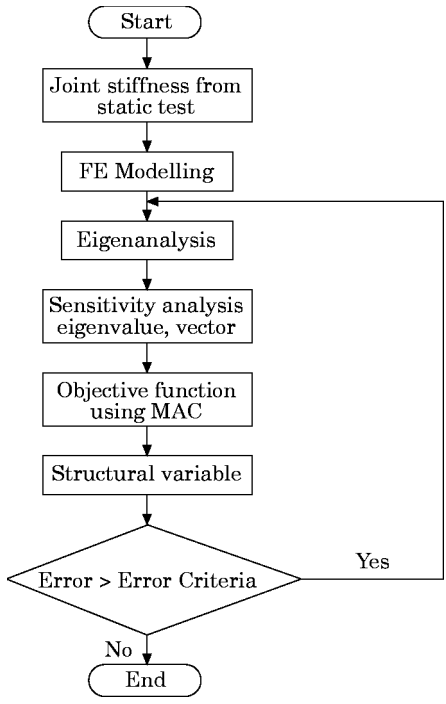

Figure 4. Updating algorithm.

From equation (10), the third term of equation (12) vanishes. The second term should be 1, if the eigenvector is mass orthonormalized. Then, the eigenvalue derivative is

$$\partial\lambda_r/\partial P_i = \{\boldsymbol{\phi}\}_r^{\mathrm{T}}(\partial[\mathbf{K}]/\partial P_i - \lambda_r\,\partial[\mathbf{M}]/\partial P_i)\{\boldsymbol{\phi}\}_r. \tag{13}$$

2.4. SENSITIVITY ANALYSIS—EIGENVECTOR DERIVATIVE

Equation (11) can be reformulated as

$$([\mathbf{K}] - \lambda_r[\mathbf{M}])\,\partial\{\boldsymbol{\phi}\}_r/\partial P_i = -(\partial[\mathbf{K}]/\partial P_i - \lambda_r\,\partial[\mathbf{M}]/\partial P_i - (\partial\lambda_r/\partial P_i)[\mathbf{M}])\{\boldsymbol{\phi}\}_r. \tag{14}$$

For simplicity, equation (14) is rewritten as

$$[\mathbf{G}]\,\partial\{\boldsymbol{\phi}\}_r/\partial P_i = \{\mathbf{f}\}, \tag{15}$$

where the rank of $[\mathbf{G}]$ is $n-1$, and $\{\boldsymbol{\phi}\}_r$ is the null-space of $[\mathbf{G}]$. Therefore,

$$[\mathbf{G}]\{\boldsymbol{\phi}\}_r = \{\mathbf{0}\} \tag{16}$$

Let $\{\boldsymbol{\sigma}\}$ be the solution of equation (15), thus

$$[\mathbf{G}]\{\boldsymbol{\sigma}\} = \{\mathbf{f}\}. \tag{17}$$

Then, $\{\boldsymbol{\sigma}\} + \gamma\{\boldsymbol{\phi}\}_r$ is also a solution, where γ is an arbitrary real number.

$$[\mathbf{G}](\{\boldsymbol{\sigma}\} + \gamma\{\boldsymbol{\phi}\}_r) = \{\mathbf{f}\}, \qquad (\because [\mathbf{G}]\gamma\{\boldsymbol{\phi}\}_r = \{\mathbf{0}\}). \tag{18}$$

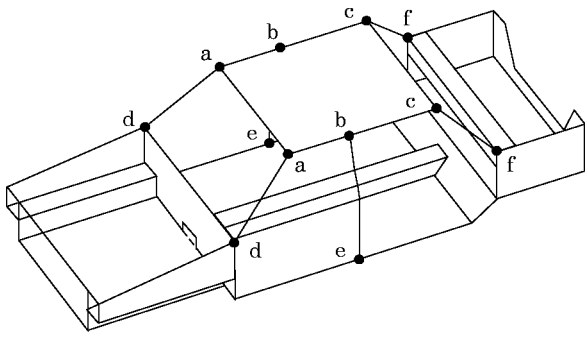

Figure 5. Automotive structural model and joints.

The solution for the eigenvector derivative is

$$\partial\{\boldsymbol{\phi}\}_r/\partial P_i = \{\boldsymbol{\sigma}\} + \gamma\{\boldsymbol{\phi}\}_r \tag{19}$$

Equation (16) can be partitioned as

$$\begin{bmatrix} [\mathbf{G}]_{jj} & \{\mathbf{G}\}_{jp} & [\mathbf{G}]_{nj}^{\mathrm{T}} \\ \{\mathbf{G}\}_{jp}^{\mathrm{T}} & G_{pp} & \{\mathbf{G}\}_{np}^{\mathrm{T}} \\ [\mathbf{G}]_{nj} & \{\mathbf{G}\}_{np} & [\mathbf{G}]_{nn} \end{bmatrix} \begin{Bmatrix} \{\boldsymbol{\phi}\}_j \\ \phi_p \\ \{\boldsymbol{\phi}\}_n \end{Bmatrix} = \begin{Bmatrix} \{\mathbf{0}\} \\ 0 \\ \{\mathbf{0}\} \end{Bmatrix}, \tag{20}$$

where ϕ_p is the pivot element. To eliminate the pth row and column, move the pth column in equation (20) to the right side giving

$$\begin{bmatrix} [\mathbf{G}]_{jj} & [\mathbf{G}]_{nj}^{\mathrm{T}} \\ \{\mathbf{G}\}_{jp}^{\mathrm{T}} & \{\mathbf{G}\}_{np}^{\mathrm{T}} \\ [\mathbf{G}]_{nj} & [\mathbf{G}]_{nn} \end{bmatrix} \begin{Bmatrix} \{\boldsymbol{\phi}\}_j \\ \{\boldsymbol{\phi}\}_n \end{Bmatrix} = -\phi_p \begin{Bmatrix} \{\mathbf{G}\}_p \\ G_{pp} \\ \{\mathbf{G}\}_{np} \end{Bmatrix}. \tag{21}$$

In equation (21), the rank of the left matrix ($n \times (n-1)$ dimension) is $n-1$, and the pth row of the matrix can be represented by a linear combination of the remaining $n-1$ rows.

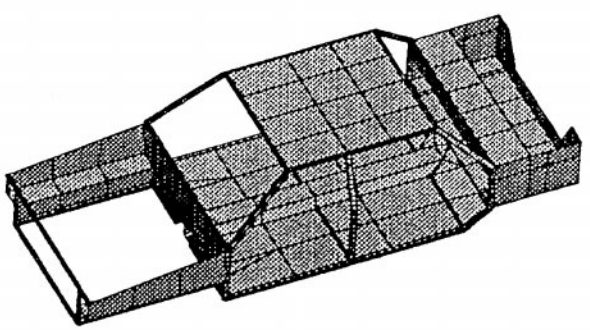

Figure 6. FE model of automotive structural model.

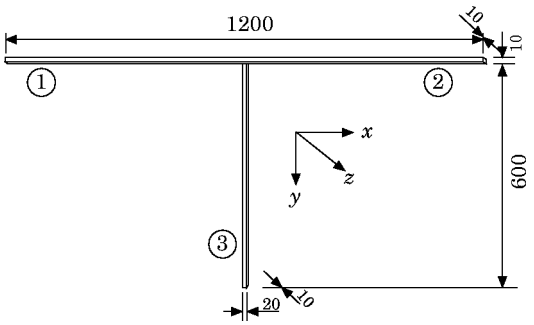

Figure 7. T-type joint.

Therefore, equation (21) can be reformulated

$$\begin{bmatrix} [\mathbf{G}]_{jj} & [\mathbf{G}]_{nj}^{\mathrm{T}} \\ [\mathbf{G}]_{nj} & [\mathbf{G}]_{nn} \end{bmatrix} \begin{Bmatrix} \{\boldsymbol{\phi}\}_j \\ \{\boldsymbol{\phi}\}_n \end{Bmatrix} = -\phi_p \begin{Bmatrix} \{\mathbf{G}\}_{jp} \\ \{\mathbf{G}\}_{np} \end{Bmatrix}. \tag{22}$$

Let the left side matrix be

$$\begin{bmatrix} [\mathbf{G}]_{jj} & [\mathbf{G}]_{nj}^{\mathrm{T}} \\ [\mathbf{G}]_{nj} & [\mathbf{G}]_{nn} \end{bmatrix} \equiv [\mathbf{g}]. \tag{23}$$

Likewise, equation (17) becomes

$$\begin{Bmatrix} \{\boldsymbol{\sigma}\}_j \\ \{\boldsymbol{\sigma}\}_n \end{Bmatrix} = [\mathbf{g}]^{-1} \left(-\sigma_p \begin{Bmatrix} \{\mathbf{G}\}_{jp} \\ \{\mathbf{G}\}_{np} \end{Bmatrix} + \begin{Bmatrix} \{\mathbf{f}\}_j \\ \{\mathbf{f}\}_n \end{Bmatrix} \right). \tag{24}$$

Choosing vector $\{\boldsymbol{\sigma}\}$ where σ_p is 0. Then equation (24) can be rewritten as

$$\begin{Bmatrix} \{\boldsymbol{\sigma}\}_j \\ \{\boldsymbol{\sigma}\}_n \end{Bmatrix} = [\mathbf{g}]^{-1} \begin{Bmatrix} \{\mathbf{f}\}_j \\ \{\mathbf{f}\}_n \end{Bmatrix}, \qquad \{\boldsymbol{\sigma}\} = \begin{Bmatrix} \{\boldsymbol{\sigma}\}_j \\ 0 \\ \{\boldsymbol{\sigma}\}_n \end{Bmatrix}. \tag{25}$$

TABLE 1

Static load test results of T-type joint (*mm*)

Moment		Measuring point ①	Measuring point ②	Distance
M_{1-2}	X	−0·135	−0·44	15
	Y	1·753	1·5875	12
	Z	1·008	1·1975	12
M_{1-3}	X	−0·18	0·138	10
	Y	1·638	1·7725	13
	Z	2·0275	2·3225	12

TABLE 2

Static load test results of edge-type joint (mm)

Moment		Measuring point ①	Measuring point ②	Distance
M_{2-1}	X	−1·42	−1·232	14·5
	Y	−0·14	0·138	13·5
	Z	−0·011	0·16	6·5
M_{2-3}	X	−0·09	−0·25	9
	Y	−0·0212	0·122	7·5
	Z	1·518	1·356	11

To calculate γ take the partial derivative of the orthonormal relationship ($\{\boldsymbol{\phi}\}_r^{\mathrm{T}}[\mathbf{M}]\{\boldsymbol{\phi}\}_r = 1$) with respect to structural variable to give

$$2(\partial\{\boldsymbol{\phi}\}_r^{\mathrm{T}}/\partial P_i)[\mathbf{M}]\{\boldsymbol{\phi}\}_r + \{\boldsymbol{\phi}\}_r^{\mathrm{T}}(\partial[\mathbf{M}]/\partial P_i)\{\boldsymbol{\phi}\}_r = 0. \tag{26}$$

Substituting equation (19) into equation (26), the arbitrary real number γ is

$$\gamma = -\tfrac{1}{2}(2\{\boldsymbol{\phi}\}_r^{\mathrm{T}}[\mathbf{M}]\{\boldsymbol{\sigma}\} + \{\boldsymbol{\phi}\}_r^{\mathrm{T}}\,\partial[\mathbf{M}]/\partial P_i\{\boldsymbol{\phi}\}_r). \tag{27}$$

Substituting equation (25) and equation (27) into equation (19) gives the complete solution of the eigenvector derivative. This method uses only a few modes that are of interest. Therefore, the required time is far less than the modal method. For more accurate calculations, it is recommended the largest possible pivot element of the eigenvector be chosen.

2.5. UPDATING ALGORITHM

In updating the structural variables, the objective function should be composed of eigenvalues and eigenvectors, and the structural variables are the stiffness values of the joints. To avoid local minima, the initial values should be close to real values. If the initial value is meaningless, the result will not be meaningful either. In this study, the initial value is obtained from static load test data and follows

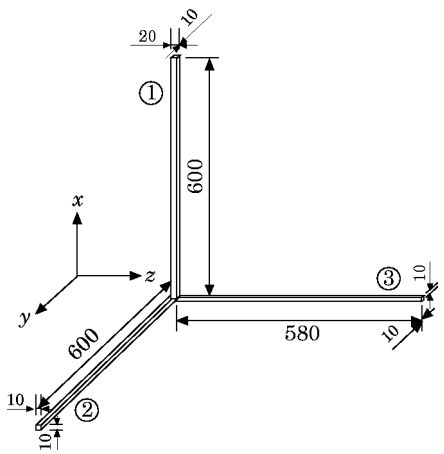

Figure 8. Edge type joint.

TABLE 3

Joint stiffness values of T-type joint ($\times 10^2$ *Nm/rad*)

	Static load test			Sensitivity analysis		
	X	*Y*	*Z*	*X*	*Y*	*Z*
K_a	1·0299	6·5236	1·3130	1·0299	7·1932	6·9321
K_b	3·5105	3·9578	4·5570	3·5105	8·0469	7·7904
K_c	3·5105	3·9578	4·5570	3·5105	5·4098	8·1500

the process explained previously. If $\omega_1, \omega_2, \ldots, \omega_n$ and $\{\boldsymbol{\phi}\}_1, \{\boldsymbol{\phi}\}_2, \ldots, \{\boldsymbol{\phi}\}_n$ are the natural frequencies and the eigenvectors which are obtained from experimental modal analysis, then, the ith eigenvalue is $\lambda_i = (2\pi\omega_i)^2$. If the objective function $\{\mathbf{h}\}$ is composed of ℓ eigenvalues and m eigenvectors, then

$$\{\mathbf{h}\} = \lfloor \lambda_1, \lambda_2, \ldots, \lambda_\ell, \{\boldsymbol{\phi}\}_1^{\mathrm{T}}, \{\boldsymbol{\phi}\}_2^{\mathrm{T}}, \ldots, \{\boldsymbol{\phi}\}_m^{\mathrm{T}} \rfloor^{\mathrm{T}}. \tag{28}$$

Equation (28) is a function of the structural variable P_i. It can be written in the form of a Taylor series expansion with respect to P_i, where $\overline{P}_i$ is the initial value.

$$\{h(P_1, P_2, \ldots, P_N)\} = \{h(\overline{P}_1, \overline{P}_2, \ldots, \overline{P}_N)\} + \sum_{i=1}^{N} \frac{\partial\{\mathbf{h}\}}{\partial P_i}(P_i - \overline{P}_i) + \sum_{i=1}^{N} \frac{\partial^2\{\mathbf{h}\}}{\partial P_i^2}(P_i - \overline{P}_i)^2 + \cdots. \tag{29}$$

Neglecting second order and higher terms,

$$\{\Delta\mathbf{h}\} = (\partial\{\mathbf{h}\}/\partial\{\mathbf{P}\}^{\mathrm{T}})\{\Delta\mathbf{P}\} \tag{30}$$

the difference of structural variable $\{\Delta\mathbf{P}\}$ is obtained as

$$\{\Delta\mathbf{P}\} = [\partial\{\mathbf{h}\}/\partial\{\mathbf{P}\}^{\mathrm{T}}]^{-1}\{\Delta\mathbf{h}\}. \tag{31}$$

The dimensions of the structural variables and objective functions are generally different. Therefore, the rank of the matrix is less than the dimension of structural variables. In this study, the pseudo inverse method using SVD (Singular Value Decomposition) is used [10]. Figure 4 shows a flow chart using the updating algorithm.

TABLE 4

Joint stiffness values of edge-type joint ($\times 10^2$ *Nm/rad*)

	Static load test			Sensitivity analysis		
	X	*Y*	*Z*	*X*	*Y*	*Z*
K_a	2·3759	3·5235	4·9993	9·2717	5·6799	5·3871
K_b	5·1807	3·1432	1·4090	6·0082	26·520	5·0943
K_c	5·1807	1·6946	3·1882	6·0077	5·6119	4·5763

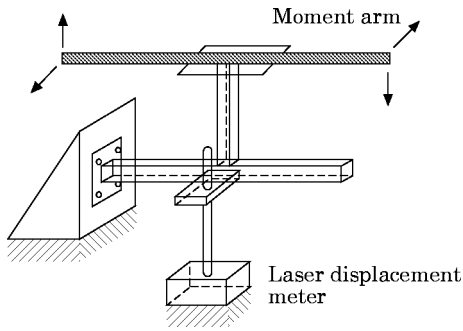

Figure 9. Experimental setup of static load test.

3. JOINT MODELLING OF AUTOMOTIVE STRUCTURAL MODEL

3.1. AUTOMOTIVE STRUCTURAL MODEL

To verify the method presented in this study, a half scale automotive structural model was fabricated. Figure 5 shows a schematic diagram of the model, where ● marks (a–f) indicate the joints. The pillars are 20×10 mm, 1 mm thick rectangular stainless steel pipe, and the other beam members are 10×10 mm and 15×15 mm, 1 mm thick rectangular pipe. The plate parts are 1·2 mm thick steel plates.

For the FE modelling and analysis, commercial code ANSYS is used. The pipes are modelled by beam element (BEAM4) and the plates are modelled by shell element (SHELL63). Figure 6 shows the FE model of the half scale automotive structural model. In Figure 6, 127 shell elements and 128 beam elements are used, and 1248 total DOF.

3.2. JOINTS OF THE AUTOMOTIVE STRUCTURAL MODEL

There are 6 kinds of joints in the automotive structural model. They can be divided into two typical joint types, T-type and edge-type. T-type joints are b and e and edge-type joints are a, c, d and f in Figure 5. In this study, roof rail joints and pillar joints that may be more flexible than other joints are chosen, and fabricated. Figures 7 and 8 show the shape of their dynamic model. Figure 9 shows the experimental setup of the static load test. To eliminate the effect of deflection of branches, short branch (200 mm long) models are made for the static load test. In order to measure rotational displacement, a 900 mm moment arm and two 1 kg

TABLE 5

Natural frequencies of T-type joint (Hz)

			Spring joint model	
Mode	Experiment	Rigid joint model	Static load test	Sensitivity analysis
1	33·78	39·68	24·69	33·78
2	34·44	45·61	31·38	34·44
3	40·02	45·65	36·99	40·02

TABLE 6

Natural frequencies of edge-type joint (Hz)

Mode	Experiment	Rigid joint model	Spring joint model	
			Static load test	Sensitivity analysis
1	29·24	36·33	27·20	29·76
2	32·44	39·30	29·42	32·67
3	41·15	46·25	35·39	38·84

weights are used. The displacement of the joint is measured with a laser displacement meter at each measuring point. The test results of each model are shown in Tables 1 and 2. In each Table, points ① and ② represent adjacent

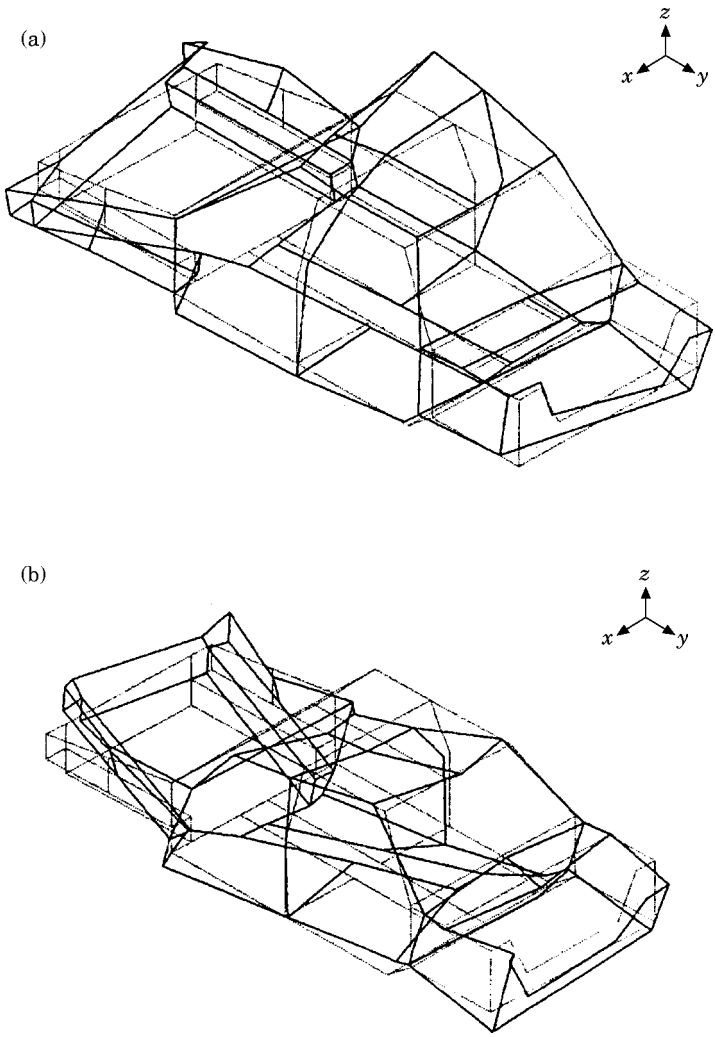

Figure 10. Experimental mode shape of automotive structural model. (a) first mode, 24·57 Hz; (b) second mode, 25·16 Hz.

TABLE 7

Natural frequencies of automotive structural model (Hz)

Mode	Experiment	Rigid joint model	Spring joint model: Static load test	Spring joint model: Sensitivity analysis	Mode shape
0	–	29·11	–	–	Local bending of the roof
1	24·57	30·72	24·15	26·02	First torsion
2	25·61	33·18	25·03	26·21	First bending
3	32·04	–	27·73	30·24	Second torsion
4	33·57	40·30	34·87	36·48	Torsion + bending

measuring points. Therefore, the rotational displacement was acquired by the difference of the linear displacement of two measuring points divided by their distance. The impulse response test of models shown in Figures 7 and 8 was performed with free–free boundary conditions. Analysis of experimental data was performed with the modal analysis program, LMS CADA-X.

Tables 3 and 4 show identified joint stiffness values that were acquired by the static load test and updating procedure with sensitivity analysis. In Tables 3 and

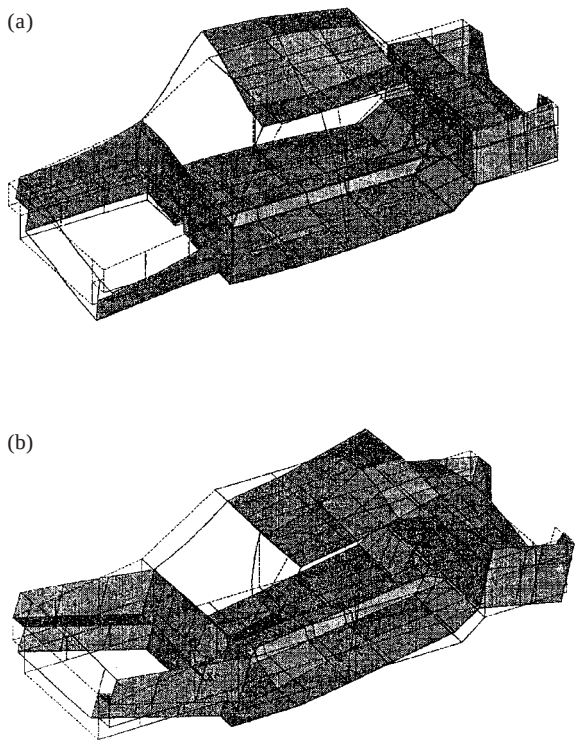

Figure 11. FE mode shape of automotive structural model. (a) first mode, 24·15 Hz; (b) second mode, 25·03 Hz.

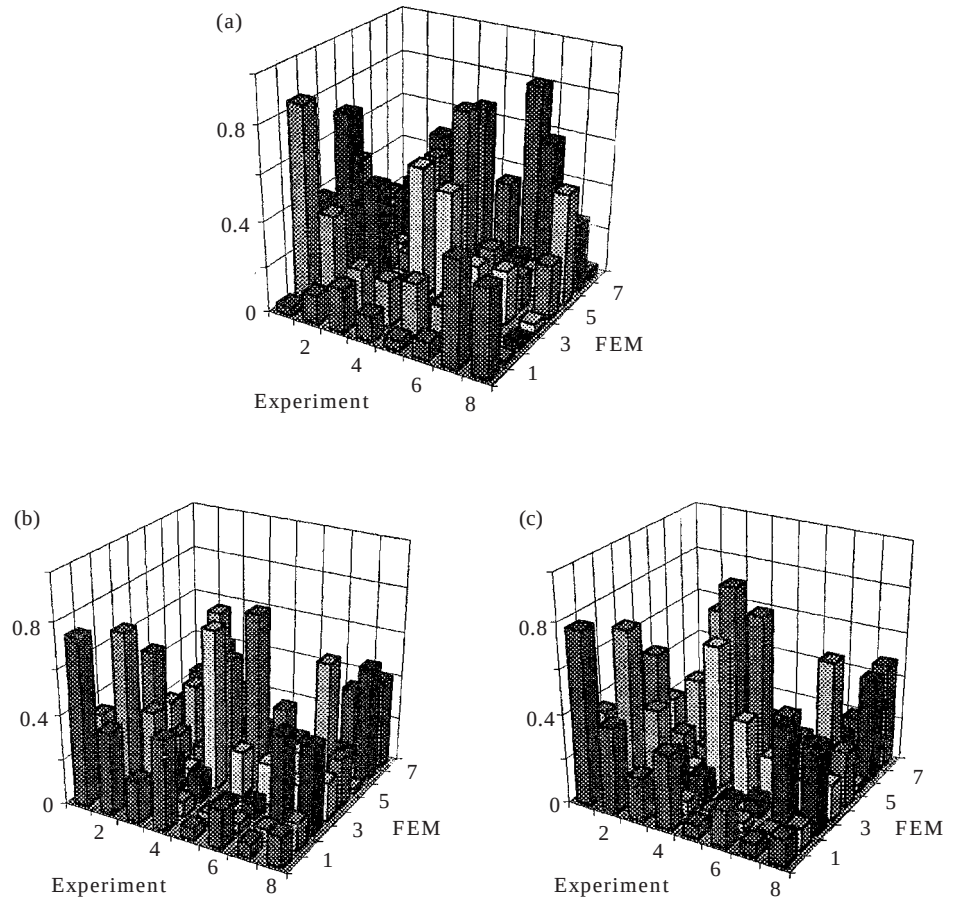

Figure 12. Comparison of MAC values. (a) Experiment and rigid joint model; (b) Experiment and spring joint model (static load test); (c) Experiment and spring joint model (sensitivity analysis).

4, joint stiffness values obtained from static load tests were smaller than that obtained from the sensitivity analysis because the procedure through static load test does not consider deflection of a branch itself. This error is negligible since the branch is short enough. The eigenvalues and eigenvectors from the experiment are used as objective values in the sensitivity analysis.

Tables 5 and 6 present natural frequencies for the experiment and each model, i.e., rigid joint model and spring joint model. In the Tables, the experiment implies impact test results, the rigid joint model implies FE analysis result that used beam elements with rigid joints, and the joint model implies the FE analysis results that used beam elements with rotational spring joints. Two types of joint stiffness values are used in the joint model. One is obtained from the static load testing and the other is obtained from sensitivity analysis. Each Table shows that natural frequencies of the rigid model are higher than others.

3.3. ANALYSIS RESULTS OF AUTOMOTIVE STRUCTURAL MODEL

The joint stiffness values in Tables 3 and 4 are applied to the half scale automobile FE model, and analysis is performed numerically and experimentally. Figure 10 shows mode shapes and natural frequencies obtained from experimental analysis. Figure 11 shows results of the FE analysis in which joints are modelled by rotational springs and the stiffness values are obtained by the static load test.

Table 7 shows the natural frequencies of each model. Figure 12 shows MAC (Modal Assurance Criterion) values of each model versus experimental results. In the case of the rigid joint model, the rigid joint shifted the first torsional frequency to a higher value. The first torsional mode is 30·72 Hz, and it is 25% higher than that of the experimental result. As shown in Figure 12(a), the first mode of the rigid joint model is local bending of the roof caused by over-stiff joints. In the case of the rotational spring joint model, in which joint stiffness values are obtained from the static load test, the first torsional frequency (24·15 Hz) is slightly lower than that in the experimental results. The natural frequencies are generally shifted lower. As shown in Figure 12(b), diagonal terms of the spring joint model are more dominant than in the rigid joint model. In the rotational spring joint model case in which joint stiffness values are obtained from sensitivity analysis, the first torsional frequency (26·02 Hz) is 5·9% higher than that of the experimental frequency. As shown in Figure 12(c), the local mode that can be found in the rigid joint model disappears and the MAC value is similar to Figure 12(b).

4. CONCLUSIONS

In this study, a methodology for modelling joints and calculating analytical stiffness values using static load test data has been proposed, and the model has been verified by comparing analysis results of the half size automotive structural FE model using both rigid joints and rotational spring joints. From the comparison of the dynamic characteristics between the experimental results and the various analytical results, the FE model in which the joint was modelled by rotational springs resulted in more accurate dynamic characteristics than the rigid joint model. Analytical joint stiffness values obtained from the proposed method is appropriate as an initial value of the updating algorithm.

REFERENCES

1. D. C. Chang 1974 *SAE Transactions* 740041. Effects of flexible connections on body structural response.
2. C. T. Chon 1986 *AIAA Journal* **25**, 1391–1395. Sensitivity of total strain energy of a local joint stiffness.
3. K. Sakurai and Y. Kamada 1988 *SAE Transactions* 880550. Structural joint stiffness of an automotive body.
4. K. Shimomaki 1990 *JSAE Transactions* **43**, 138–142. Joint stiffness of body structures: part 1—its evaluation method (in Japanese).
5. K. J. Lee 1992 *Ph.D. Thesis*, *Virginia Polytechnic Institute and University*. Modelling and identification of flexible joints in vehicle structures.

6. R. L. Fox and M. P. Kapoor 1968 *AIAA Journal* **6**, 2426. Rates of change of eigenvalues and eigenvectors.
7. K. Sohn 1992 *Ph.D. Thesis*, *Tokyo Institute of Technology*. A study on finite-element modelling of mechanical structures for vibration analysis.
8. R. B. Nelson 1976 *AIAA Journal* **14**, 1201–1205. Simplified calculation of eigenvector derivatives.
9. M. K. Lim and R. N. Lin 1993 *IMAC XI*. 1554–1558. Method for calculating derivatives of eigenvalues and eigenvectors.
10. G. Strang 1988 *Linear Algebra and Its Applications*. HBJ.